Thin Solid Films 565 (2014) 149–154

Contents lists available at ScienceDirect

Thin Solid Films

journal homepage: www.elsevier.com/locate/tsf

Influence of the atmospheric species water, oxygen, nitrogen and carbon dioxide on the degradation of aluminum doped zinc oxide layers

Mirjam Theelen [a,b,*], Supratik Dasgupta [a], Zeger Vroon [a], Bas Kniknie [a], Nicolas Barreau [c], Jurgen van Berkum [d], Miro Zeman [b]

[a] TNO, Thin Film Technology, High Tech Campus 21, 5656 AE Eindhoven, The Netherlands
[b] Delft University of Technology, Photovoltaic Materials and Devices, Mekelweg 4, 2628 CD Delft, The Netherlands
[c] Institut des Matériaux Jean Rouxel (IMN)-UMR 6502, Université de Nantes, CNRS, 2 rue de la Houssinière, BP 32229, 44322 Nantes Cedex 3, France
[d] Philips Innovation Services, High Tech Campus 11, 5656 AE Eindhoven, The Netherlands

ARTICLE INFO

Article history:
Received 12 March 2014
Received in revised form 2 July 2014
Accepted 2 July 2014
Available online 9 July 2014

Keywords:
CO_2
Degradation
Diffusion
Grain boundaries
Water
Zinc oxide
ZnO:Al

ABSTRACT

Aluminum doped zinc oxide (ZnO:Al) layers were exposed to the atmospheric gases carbon dioxide (CO_2), oxygen (O_2), nitrogen (N_2) and air as well as liquid H_2O purged with these gases, in order to investigate the chemical degradation behavior of these layers. The samples were analyzed by electrical, compositional and optical measurements before, during and after exposure to these conditions in order to follow the degradation behavior of these layers in time.

We have shown that ZnO:Al layers degraded in the presence of a mixture of H_2O and CO_2. Individually, CO_2 does not impact the degradation at all during the tested period, while the individual impact of H_2O is small. However, when CO_2 is also present, the concentration of OH increases greatly in the bulk and even more at the air/ZnO:Al and in the ZnO:Al/glass interfaces. Carbon based species are then also present, indicating that $Zn_5(OH)_6(CO_3)_2$ is also formed at the grain boundaries. The impact of gaseous O_2 as well as water purged with N_2 and O_2 on ZnO:Al degradation is very small.

1. Introduction

Zinc oxide (ZnO) has been investigated extensively because of the increasing number of commercial applications. Being a wide band gap semiconductor ($E_g = 3.4$ eV), doped ZnO is emerging as a prospective material for among other gas sensors, electronics and thin film solar cells, such as $Cu(In,Ga)Se_2$. For the latter, aluminum doped ZnO (ZnO:Al) is often used as the front contact. It is known that the ingression of H_2O in this material leads to decreased device performance [1]. This effect is normally minimized by the use of encapsulated products which are often optimized to function as a barrier for water [2].

In order to choose the best required barrier product, based on costs and product performance, it is necessary to understand and limit the degradation behavior of ZnO:Al. This is often obtained according to certification standard IEC 61646, which contains among others the 'damp heat' test. This test (1000 h exposure to 85 °C and 85% Relative Humidity (RH)) can help in the identification of reliability problems in the material and can give an indication of its field performance. Several studies [3–9] have used damp heat testing, which has led to an increased insight of the changes in the optical and electrical properties during degradation. However, the degradation mechanisms as well as the chemical reactions leading to the change in properties are still largely unknown.

Furthermore, it is expected that other atmospheric species like O_2 or CO_2 might also play a role in the degradation, but this has not been studied thoroughly. The exact nature of the environmental molecules that are playing a role in the relevant degradation processes in ZnO:Al is proposed in literature, but has not been studied thoroughly. A suggestion for the main degrading species includes oxygen and water molecules [7] and water and CO_2 [9].

Knowledge about the species playing a role in ZnO:Al degradation is very important, because it can be used to optimize the product design for ZnO:Al containing products. This can for example be useful in the design of encapsulation materials in which the water and oxygen barrier properties (water vapor transmission rate and oxygen transmission rate respectively) are optimized, while the penetration of other atmospheric species is not defined at all.

In this study, we studied the impact of the exposure of thin film ZnO:Al to these atmospheric species (N_2, O_2, CO_2, H_2O), in order to learn more about the influence of these species and their combination on the degradation.

* Corresponding author at: TNO, Thin Film Technology, High Tech Campus 21, 5656 AE Eindhoven, The Netherlands.
E-mail address: mirjam.theelen@tno.nl (M. Theelen).

http://dx.doi.org/10.1016/j.tsf.2014.07.005
0040-6090/

2. Experimental

2.1. Sample preparation

ZnO:Al layers were deposited by radio frequency (rf) magnetron sputtering using a MRC 643 vertical batch sputtering tool. The layers were sputtered on a 10 × 10 cm^2 0.7 mm thick Eagle 2000 Corning glass substrate from a rectangular 5″ × 17″ high purity ZnO ceramic target with 2% Al_2O_3. The flow of pure Ar gas was set to 15 standard cubic cm^2 per minute. The chamber pressure was 0.42 Pa, while the rf power was 800 W, which corresponds to a power density of 1.46 W/cm^2. The deposition time was 35 min and was executed in 14 passes. The deposition was executed at room temperature.

2.2. Sample degradation

All samples in this study were obtained from one 10 × 10 cm^2 substrate with a ZnO:Al coating, which was cut into smaller samples. The initial thickness and sheet resistance measured over the complete sample had standard deviation of 5%. The water samples were placed in closed vessels, which were filled with 150 mL ultrapure water (demineralized water further treated by a Synergy Millipore tool). One vessel only contained water in an open connection to the atmosphere, while the other vessels were purged with the gases O_2 (purity: 99.995%), N_2 (purity: 99.99995%), CO_2 and compressed air (Fig. 1). It is expected that purging the water with the gases will lead to the presence of only water and gas, while no additional species are present, except for species that might have dissolved from the glass or the ZnO:Al layer. For water without purging, it is expected that all species present in the atmosphere are dissolved in water in small quantities.

The gas samples were placed in CO_2 and O_2 atm, while reference samples were kept in an argon glovebox (MBraun glovebox Unilab). All the samples were removed from the vessels at set times and analyzed. For the samples in the water vessels, these degradation periods took 4/4/4/4/4/6/6/6/6/6/17/17/17/17/17/17/17/17/17/17/20/20/20/20 h, which counted up to 310 h. The pH of the water in the vessels was checked before the removal of the samples, to observe whether the pH has changed. The samples in the gaseous O_2 and CO_2 were kept up to 1000 h under these conditions.

In Table 1, names used in this article to refer to the ZnO:Al samples and the conditions of the degradation experiments of the samples are summarized.

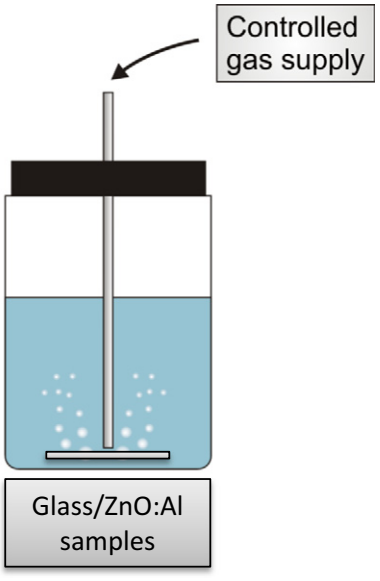

Fig. 1. Schematic picture of the degradation setup.

Table 1
Degradation conditions for the ZnO:Al samples and the name they are referred to in this article.

Conditions	Name
H_2O	H_2O
H_2O purged with CO_2	H_2O/CO_2
H_2O purged with O_2	H_2O/O_2
H_2O purged with N_2	H_2O/N_2
H_2O purged with compressed air	H_2O/air
CO_2 gas	CO_2
O_2 gas	O_2
Argon gas (glovebox)	Argon

2.3. Characterization of film properties

The optical, structural and electrical properties were determined by a number of techniques before, during and after degradation.

A PhysTech RH2010 Hall effect measurement tool was used to determine the electrical properties of the layers. The optical properties were determined by a Shimadzu UV-3600 UV-VIS-NIR, which allowed analysis of the transmittance and reflectance of the ZnO:Al samples including glass. From these data, the absorption is calculated. A Leica Wild M400 macroscope and a digital camera were used to determine the visual changes.

The morphological and structural properties of the layers were determined by a FEI Quanta 600 Scanning Electron Microscope (SEM) combined with Energy Dispersion X-ray (EDX) EDAX Genesis 4000, and a Zeiss Orion plus Helium Ion Microscope (HIM) with an Everhart–Thornley detector. The He ions have a voltage of 25 kV with a current of 0.5 to 2 pA. A Philips X'pert 5068 powder diffractometer, equipped with a CuK_α ($\lambda = 0.154$ nm) source in the 5° to 95° 2θ range with a step size of 0.02° was also used to determine the structural properties.

Time-Of-Flight Secondary Ion Mass Spectrometry (TOF-SIMS) depth profiling was performed using an Ion-Tof TOF-SIMS IV instrument, operated in negative mode, using high current 25 keV Bi^+ beam of ~3 μm diameter for analysis and 2 keV Cs^+ ions for sputtering.

3. Results

3.1. Structural properties

From cross section HIM and SEM pictures, it was concluded that the non-degraded ZnO:Al layer has a columnar structure and a thickness of 480–520 nm It was observed that the structure of the columns was not completely straight, but showed a wavy structure. This wavy structure can be caused by the movement of the substrate during deposition on the semi-industrial tool, which slowly moves the substrate back and forth during the deposition.

During degradation, the most striking observation was complete dissolution of the sample that was placed in H_2O purged with CO_2, which occurred within hours. No further results of this sample are therefore given in this article. The other samples did not dissolve and their compositional, optical and electrical properties were followed for 310 h.

After exposure to most treatments, no differences in structural properties could be observed. The structure of the H_2O/N_2 sample is shown in Fig. 2 as an example. However, an unexpected change in morphology was observed for the H_2O/air sample, in which gaps occurred in the ZnO:Al layer at the glass interface (Fig. 2), indicating local dissolution of the ZnO:Al. It was observed that only the bottom 200 nm was affected, while the top part of the ZnO:Al still looked intact. This was not expected, since the water and other reactive species are initially only present at the top of the ZnO:Al layer. This effect was not unambiguously shown for the non-purged H_2O, but probably also occurred.

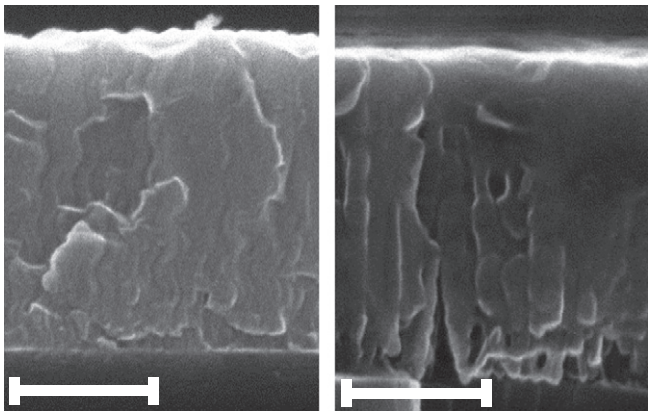

Fig. 2. Cross section HIM pictures after degradation: Left: ZnO:Al H_2O/N_2 sample; Right: ZnO:Al H_2O/air with gaps near the glass/ZnO:Al interface. The scale bars indicate 250 nm.

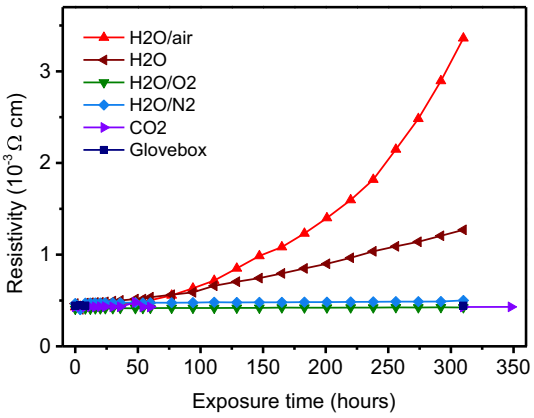

Fig. 3. Development of the resistivity of ZnO:Al as a function of exposure time to the various conditions.

When the samples were studied by eye or by macroscope, it was observed that most samples did not look significantly different after degradation, although the H_2O/air sample looked less homogeneous.

X-Ray Diffraction (XRD) measurements showed that the ZnO:Al samples before degradation had a polycrystalline wurtzite structure and consisted of hexagonal crystallites with a strong preferred orientation in the (002) directions along the c-axis perpendicular to the substrate. The (004) orientation was also observed. Apart from the dissolved sample exposed to H_2O/CO_2, the degradation neither led to the introduction of any additional signals nor led to a significant change in position or shape of the signals. Furthermore, the structural properties of the all the ZnO:Al samples were constant.

3.2. Electrical properties

Hall measurements showed that before degradation, all samples had a sheet resistance of 10.0 ± 0.5 Ω/□, corresponding to a resistivity of 4.5–5 × 10^{-4} Ωcm. Clear differences in the evolution of the resistivity as a function of exposure time were observed for the samples exposed to different atmospheric gases (Fig. 3). During exposure, no change in resistivity was observed for the samples stored under an argon or a gaseous O_2 or CO_2 atmosphere, while the samples exposed to water purged with nitrogen and oxygen showed a very slow increase. This was especially visible during the first thirty hours, and continued very slowly for the following 300 h. A larger impact was observed for the samples that were stored in water without purging, therefore naturally containing some atmospheric gases. This sample showed a twofold increase over 210 h of exposure time. The H_2O/air showed the largest increase, which resulted in a sheet resistance of over 80 Ω/□ after 310 h.

The main reason for the increase in resistivity could be found in the electron mobility (Fig. 4). For the samples stored in CO_2 and in water purged with N_2 and O_2, a small initial decrease in the first 100 h was observed, followed by a stable electron mobility. The samples exposed to water with or without compressed air showed a very large decrease in this electron mobility.

A minor change in electrical properties was also visible in the carrier concentration of the samples in water and water purged with compressed air (Fig. 3). This effect was small compared to the change in electron mobility. The samples stored in water purged with nitrogen and oxygen as well as the samples stored in a CO_2 atm did not show any decrease in the carrier concentration.

3.3. Optical properties

In Fig. 5 the optical properties determined by UV–VIS measurements of the samples after exposure to H_2O/O_2 and H_2O with and without purging are shown. The optical properties of H_2O/N_2 are very similar to the H_2O/O_2 sample. In these graphs, it can be observed that the optical parameters of the H_2O/O_2 sample barely changed with time in the measured wavelength region (240–2400 nm). For these samples, the constant plasma frequency and the constant transmission in both the near infrared and the UV region imply that the carrier concentration is constant in the bulk of the film, as is also observed in Hall measurements. The samples exposed to gases (CO_2, O_2) are not depicted but barely showed any change.

However, for the H_2O and H_2O/air samples, large changes in the optical properties were observed. For the H_2O sample, the fringes get a little bit weaker, while the transmission in the IR region slightly increases. In the region above 1500 nm, the reflection decreases while the absorption increases. For the H_2O/air sample, these effects became stronger: the fringes have completely disappeared, the transmission in the IR region has increased, while the reflection in this region decreased.

3.4. Compositional changes

The change of composition as a function of the sample depth was determined by ToF-SIMS measurements.

The intensity depth profiles of the most relevant ions of various ZnO:Al layers (non-degraded, H_2O/O_2 and H_2O/air) are shown in Fig. 6. We observed that the reference sample showed completely flat profiles of the matrix species AlO_3, ZnO and O. Furthermore, it has mostly flat profiles of the 'foreign' species OH, H, C, S, Cl and PO_x, where part of the signals may be due to instrumental background. However, in this sample, and less visible in the H_2O/O_2 sample, the OH and H contents show a 14-cycle periodic variation, as if the layer consists of 14 sublayers. It was checked under different conditions and concluded that it was not an instrumental effect. Since the samples were deposited in 14 passes in the sputtering tool, it can be concluded that H_2O or similar species are incorporated in small quantities during the deposition process.

Exposure to H_2O/O_2 seems to lead to the smoothening of the OH and H profiles in the bulk and near the glass. Furthermore, small signal increases of most 'foreign' species (OH, H, C, S, Cl and PO_x) were observed near the top of the sample. The largest concentration increase was observed for hydroxide.

The sample exposed to H_2O/air showed a completely different composition profile: much higher signals for OH, H, C, Cl, PO_x were observed (20 fold increase of OH in the bulk). These species are even more enhanced near the ZnO:Al/glass and the air/ZnO:Al interfaces. For the newly observed species S and Cu, the gradient near the interface was even steeper. At the interface regions, where the foreign species have a very high concentration, the matrix materials O, ZnO and AlO_3 show a decrease.

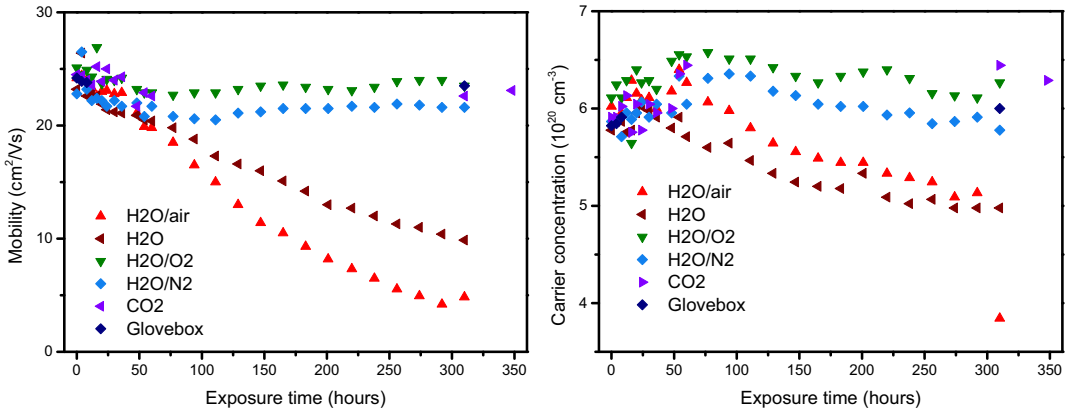

Fig. 4. Development of the mobility and the carrier concentration as a function of exposure time to the various conditions.

3.5. Acidity measurements

Since it was expected that the presence of CO_2 would impact the pH, this value was measured for the water based experiments before the removal of the samples from the H_2O vessels for analysis. It was noticed that the pH showed a small initial increase (an average from 7.9 to 8.4) followed by a slow and steady increase over the duration of the experiments, on average from 8.4 to 9.2. This effect was the strongest for the N_2 purged vessel and the smallest for the O_2 purged vessel. Another control experiment did show a small initial increase, but it did not show any later effect on the pH. The small observed changes might have resulted from the measurement error of the pH measurement tool. It can be concluded that the pH did not change more for the H_2O/air and H_2O vessels than for the H_2O/N_2 an H_2O/O_2, so large global fluctuations of the pH were not the cause of the difference in degradation behavior.

The pH of the H_2O purged with CO_2 showed a pH value of 4.7.

4. Discussion

The impact of the treatments on the ZnO:Al samples resulted in different degradation effects.

4.1. Gases

The impact of exposure of ZnO:Al to different kinds of gases (pure CO_2, O_2 and Ar) was minimal. Both the electrical and the optical properties did not change significantly. In general, it can be stated that ZnO:Al seems to be stable for middle long term exposure (up to 1000 h) to these conditions.

4.2. Water purged with nitrogen or oxygen

When the H_2O/N_2 and H_2O/O_2 samples are considered, a minor increase in resistivity during the first 100 h was observed. The electrical changes could majorly be attributed to changes in mobility, while the carrier concentration did not change significantly.

Reference [10] describes the dominant electron scattering mechanisms in zinc oxide limiting the electron mobility for ZnO:Al: potential barriers at the grain boundaries and ionized impurity scattering in the grain. For the H_2O/N_2 and H_2O/O_2 samples, based on the stable carrier concentrations and the decreasing mobility, it can be expected that the formation of detrimental compounds in zinc oxide occurs mainly at the grain boundaries and not in the bulk material.

This is supported by the observation in reference [11], which shows that neon cannot effuse through the bulk of the grains, while it can migrate through the grain boundaries. Therefore, the transport of molecules like oxygen, nitrogen and water is likely also only possible through the grain boundaries. Since the effects for H_2O/N_2 and H_2O/O_2 on both the electrical and the optical parameters are minor and nitrogen is known for its inertia, it is not expected that oxygen plays a large role in the degradation of ZnO:Al. Therefore, it is expected that the main component leading to ZnO:Al degradation under these conditions is H_2O.

Furthermore, reference [12] showed experimentally that $Zn(OH)_2$ is kinetically favored at low temperatures (under 34 °C) and can thus also be formed according to:

$$Zn^{2+}(aq) + 2OH^{-}(aq) \rightarrow Zn(OH)_2(s). \quad (1)$$

Therefore, we propose that the formation of $Zn(OH)_2$ in the grain boundaries is the driving force behind water driven mobility decrease.

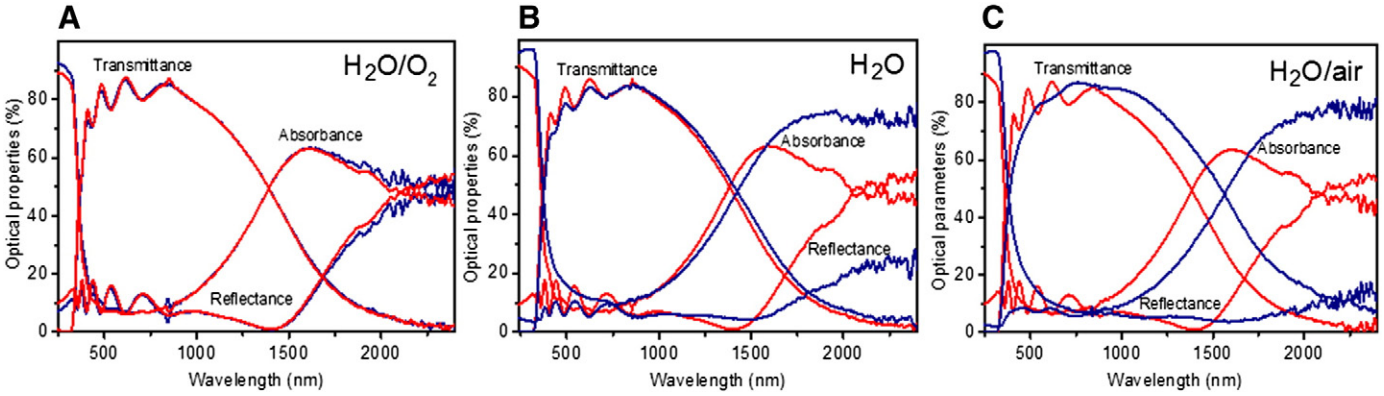

Fig. 5. Optical properties before (red) and after 310 h exposure to various conditions (blue). A: H_2O/O_2. B: non-purged H_2O. C: H_2O/air.

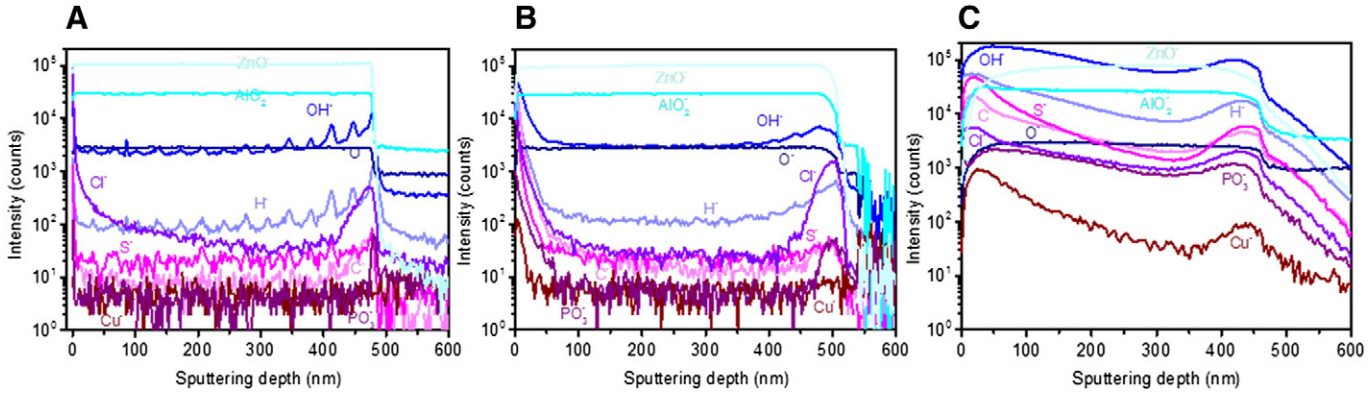

Fig. 6. SIMS depth profiling of the ZnO:Al. A: non-degraded. B: 310 h exposure to H_2O/O_2. C: 310 h exposure to H_2O/air.

4.3. Water purged with CO_2

The sample in H_2O/CO_2 dissolved directly, which is caused by the decreased pH (4.7), that occurred due to the dissolution of CO_2 in water.

$$H_2O(l) + CO_2(g) \rightarrow 2H^+(aq) + CO_3^{2-}(aq) \quad (2)$$

The chemical stability of zinc oxide in an aqueous solution is a function of pH. It is thermodynamically stable in pH between 6 and 12, outside this pH range, zinc oxide dissolves [13]. In an acidic environment, the following reaction occurs:

$$ZnO(s) + 2H^+(aq) \rightarrow Zn^{2+}(aq) + H_2O(l). \quad (3)$$

4.4. Water and water purged with air

The effect for the H_2O/air and H_2O samples is more severe than the degradation of the H_2O/N_2 and the H_2O/O_2 samples. When considering non-purged water as well as water purged by compressed air, it can be assumed that the gases found in air will be present in water. A standard air mixture contains N_2 (~78% volume), O_2 (~21%), Ar (~1%) and CO_2 (0.03% volume) plus other constituents (e.g. H_2, Ne, He, Kr) in concentrations under 20 ppm. Since ZnO:Al appears to be inert for N_2 and O_2, while Ar is known to be very inert, it is expected that the main reactive species in air is CO_2.

A possible reaction product, as also described in reference [3], is hydrozincite. Its formation from zinc hydroxide follows this reaction:

$$Zn(OH)_2(s) + 4Zn^{2+}(aq) + 4OH^-(aq) + 2CO_3^{2-}(aq) \rightarrow Zn_5(CO_3)_2(OH)_6(s). \quad (4)$$

The formation of a carbonate and hydroxide containing material is also supported by the observation of large quantities of H, OH and C in SIMS analysis. Furthermore, S and Cl were also present. As presented in reference [13], various natural degradation products of zinc contain chlorides and sulfates. These products are formed in the presence of Cl^- and SO_4^{2-} ions. The formation reactions are analog to reaction (4), and is expected to result in the formation of e.g. $Zn_5(OH)_8Cl_2 \cdot H_2O$ (zinc hydroxychloride) and $Zn_4SO_4(OH)_6 \cdot nH_2O$ (basic zinc sulfate). The origin of the 'foreign' elements was not shown, but these must have resulted either from the compressed air or glass (jar or substrate).

Another observation for the H_2O/air samples was the appearance of gaps in the ZnO:Al layer near the glass/ZnO:Al interface. This can be explained by preferred dissolution of the ZnO:Al near the interface. This indicates that ions from the glass have played a catalytic role in the etching of the ZnO:Al, for example by a local change in pH. In previous work [3], it was shown that especially silicon and calcium can migrate through the grain boundaries from borosilicate glass. Possible candidates for ions with a catalytic role are therefore for example basic SiO_3^{2-} or Ca^{2+}. Since ZnO:Al dissolves both under basic conditions (pH > 12) and acidic conditions (pH < 6), while it is stable in a pH between 6 and 12 [13], it cannot be distinguished which reaction is more likely. However, since CO_3^{2-} is probably involved, an acidic reaction is most likely to have occurred.

A significant pH change was not observed, but the volume of formed H^+ or OH^- has been very small compared to the total volume of H_2O. Therefore, a local change in pH is possible even when no significant pH shift in the H_2O has been observed.

The changes in optical properties of the H_2O/air sample compared to e.g. H_2O/O_2 can be explained by two phenomena:

1. An increased transmission from 1000–2400 nm: this can be explained by a decrease of the carrier concentration. This is supported by the change in carrier concentration as observed in the electrical measurements.
2. The disappearance of the fringes (350–950 nm) as well as decreased reflection (1700–2400 nm): this can be explained by increased scattering caused by an increased roughness of the ZnO:Al at the glass/ZnO:Al interface, due to the dissolution of ZnO:Al.

5. Conclusions

In literature, it is often stated that both H_2O and O_2 are involved in the degradation of ZnO:Al. In this study, we show that the driving force behind ZnO:Al degradation is the combined presence of H_2O and CO_2. Individually, gaseous CO_2 does not impact the degradation at all during the tested period, while the individual impact of H_2O is minor: the latter leads to slow diffusion of water down the grain boundaries, where it reacts, possibly resulting in the formation of $Zn(OH)_2$. This leads to a decrease in the electrical mobility. However, in the presence of CO_2, the electrical and optical properties change very quickly. Depth profiling showed that the concentration of OH is a factor 20 times higher in the bulk, and even higher at the air/ZnO:Al and in the ZnO:Al/glass interface, while C, H, Cl and S were also observed.

Acknowledgments

The authors would like to thank Henk Steijvers, Linda van de Peppel, Felix Stegeman, Emile van Veldhoven, Arjan Hovestad (TNO) and Bertil Okkerse (Philips Innovation Services) for their assistance with the measurements, analysis, the building of the setup or for the fruitful discussions. This study was carried out under project number M71.9.10401 in the framework of the Research Program of the Materials innovation institute (M2i) (www.m2i.nl).

References

[1] J. Wennerberg, J. Kessler, L. Stolt, Degradation mechanisms of Cu(In,Ga)Se_2 thin film PV modules, Proceedings of the 16th European PV Solar Energy Conference, Glasgow, UK, 2000, p. 309.

[2] D. Coyle, Life prediction for CIGS solar modules part 1: modeling moisture ingress and degradation, Prog. Photovolt. Res. Appl. 21 (2) (2013) 156.

[3] M. Theelen, T. Boumans, F. Stegeman, F. Colberts, A. Illiberi, J. van Berkum, N. Barreau, Z. Vroon, M. Zeman, Physical and chemical degradation behavior of sputtered aluminum doped zinc oxide layers for Cu(In, Ga)Se2 solar cells, Thin Solid Films 550 (2014) 530.

[4] E. Ando, M. Miyazaki, Durability of doped zinc oxide/silver/doped zinc oxide low emissivity coatings in humid environment, Thin Solid Films 516 (2008) 4574.

[5] T. Minami, T. Miyata, Y. Ohtani, T. Kuboi, Effect of thickness on the stability of transparent conducting impurity-doped ZnO thin films in a high humidity environment, Phys. Status Solidi Rapid Res. Lett. 1 (2007) 31.

[6] T. Tohsophon, J. Hupkes, S. Calnan, W. Reetz, B. Rech, W. Beyer, N. Sirikulrat, Damp heat stability and annealing behavior of aluminum doped zinc oxide films prepared by magnetron sputtering, Thin Solid Films 511–512 (2006) 673.

[7] W. Lin, R. Ma, J. Xue, B. Kang, RF magnetron sputtered ZnO:Al thin films on glass substrates: a study of damp heat stability on their optical and electrical properties, Sol. Energy Mater. Sol. Cells 91 (2007) 1902.

[8] D. Greiner, S. Gledhill, C. Köble, J. Krammer, R. Klenk, Damp heat stability of Al-doped zinc oxide films on smooth and rough substrates, Thin Solid Films 520 (2011) 1285.

[9] I. Hüpkes, J. Owen, M. Wimmer, F. Ruske, D. Greiner, R. Klenk, U. Zastrow, J. Hotovy, Damp heat stable doped zinc oxide films, Thin Solid Films 555 (2014) 48.

[10] J. Steinhauser, S. Meyer, M. Schwab, S. Faÿ, C. Ballif, U. Kroll, D. Borrello, Humid environment stability of low pressure chemical vapour deposited boron doped zinc oxide used as transparent electrodes in thin film silicon solar cells, Thin Solid Films 520 (2011) 558.

[11] W. Beyer, U. Breuer, F. Hamelmann, J. Hüpkes, A. Stärk, H. Stiebig, U. Zastrow, Hydrogen diffusion in zinc oxide thin films, Mater. Res. Soc. Symp. Proc. 1165 (2009) 209.

[12] A. Goux, T. Pauporté, J. Chivot, D. Lincot, Temperature effects on ZnO electrodeposition, Electrochim. Acta 50 (2005) 2239.

[13] X. Zhang, Corrosion and Electrochemistry of Zinc, Springer, 1996.